Available online at www.sciencedirect.com
ScienceDirect
Ceramics International 35 (2009) 1493–1500
CERAMICS INTERNATIONAL
www.elsevier.com/locate/ceramint

# Effect of pyrophyllite on the mullitization in triaxial porcelain system

T.K. Mukhopadhyay *, S. Ghatak, H.S. Maiti

*Central Glass & Ceramic Research Institute, Kolkata 700032, India*

Received 29 May 2008; received in revised form 9 June 2008; accepted 6 August 2008
Available online 31 August 2008

**Abstract**

China clay (kaolin) was progressively replaced by pyrophyllite in a conventional porcelain mix. Addition of 5% pyrophyllite as a replacement of china clay improved the fired strength by about 24% compared to that of the conventional body fired at 1300 °C. Percentage of mullite was found to increase in the fired specimens when kaolinite was progressively replaced by pyrophyllite. However, beyond 7.5% pyrophyllite addition, amorphous $SiO_2$ released from pyrophyllite dehydroxylate inhibited further recrystallization of mullite. There was very insignificant change in the phase compositions with mixes having pyrophyllite content higher than 7.5%. Entire phenomenon has been explained on the basis of structural reorganization of pyrophyllite during dehydroxylation. Presence of large amount of undissolved quartz of smaller size as well as isolated pores in the microstructures of specimens containing pyrophyllite more than 7.5% are assumed to hinder the propagation of crack and thereby improving the mechanical properties. The size and shape of mullite crystals is to a large extent controlled by the fluidity of the liquid matrix from which they grow and this is again a function of temperature and composition.


*Keywords:* D. Mullite; D. Porcelain; Pyrophyllite

## 1. Introduction

Pyrophyllite is a hydrous aluminium silicate ($Al_2O_3$, $4SiO_2$, $H_2O$). It resembles talc in its softness and crystal structure, but occurs less commonly in nature. The major impurities in pyrophyllite are quartz, diaspore, bauxite and mica. This mineral is extensively used as filler in rubber, roofing, soap, asbestos products and insecticide, whereas its use in ceramic industries is very much limited.

The scantiness of the reserves of ceramic raw materials has made a strong influence on the cost of final products. Efforts in research have been made for studying new materials that are able to replace the traditional ingredients without much change in the process or quality of the final products [1–3]. Technologists are taking particular interest to reformulate the body mix composition by partial or total replacement of one or more component of the natural or conventional raw materials with a readily available non-conventional or waste material [4,5]. The use of these materials is considered viable only if the industrial process essentially remains unchanged and the quality and ultimate properties of the products do not deteriorate [6–9]. Incorporation of non-conventional raw materials viz. wollastonite, talc, pyrophyllite, etc. in the batch formulations is becoming popular in order to accommodate faster firing technique as well as to reduce the maturing temperature [10,11]. Prasad et al. [12] replaced quartz and feldspar with sericitic pyrophyllite ($K_2O + Na_2O = 10.08\%$) in a whiteware composition. Incorporation of 22.5% sericitic pyrophyllite resulted in increased fired strength along with decrease in thermal expansion. This was attributed to the presence of spherical shaped pores and the decrease in free quartz content in the fired specimen. In another work of Bhasin et al. [13] the effect of pyrophyllite additions on sintering characteristics of fly ash-based ceramic wall tiles was studied. The impact strength and apparent density was found to increase with the increase in pyrophyllite content while decreased water absorption values were observed. Further, presence of pyrophyllite imparted improved thermal shock resistances. Rieger [14] observed that high-sericitic pyrophyllite has the ability to form mullite at comparatively low temperature and

* Corresponding author. Fax: +91 33 2473 0957.
*E-mail address:* tapas@cgcri.res.in (T.K. Mukhopadhyay).

0272-8842/$34.00 
doi:10.1016/j.ceramint.2008.08.002

interlocking grain structure of mullite results in greatly increased fired strength in vitrified bodies.

Most of the research workers have tried to incorporate the new material as a replacement of non-plastic components viz. quartz and feldspar in the conventional whiteware compositions. In our earlier communication [15] quartz was progressively replaced by pyrophyllite in a conventional porcelain mix with composition 50% clay, 25% quartz and 25% feldspar. In this paper we have tried to replace the costlier ingredient, i.e. china clay progressively by pyrophyllite, a cheaper aluminosilicate material. Effect of such substitution on shrinkage, bulk density, porosity, strength, phase evolution in relation to firing temperature was studied and compared with conventional whiteware mix. Some selected samples were examined for microstructural analysis.

## 2. Experimental

The raw materials used in this investigation were china clay (Rajmahal, Bihar, India), plastic clay (Ranchi, Jharkhand, India), quartz, feldspar and pyrophyllite (Maharashtra, India).

The chemical analysis of the raw materials conducted by standard method is given in Table 1.

Batch (Table 2) was wet ground for 16 h in porcelain jars with porcelain balls up to a fineness of around 53 μm. The ground slurry was sieved, passed through a permanent magnet, dewatered and dried in an oven at 120 °C. The dried mass was powdered and passed through a 150 μm sieve, moistened with 6% water and test specimens were pressed in a semi-automatic press of 5 MT capacity. Specimens were made in the form of rectangular bars of 100 mm × 15 mm and 5-mm thickness. The test specimens were dried and subsequently fired between 1150 °C and 1300 °C in an electric furnace with 2 h soaking at the respective peak temperatures.

Apparent porosity and bulk density of the specimens fired at different temperatures were measured by the water displacement method. Flexural strength in three point bending stress was measured with an electro-mechanical universal tester (Instron 5500R—Universal Testing Machine). The cross-head speed was 1 mm/min and a span of 80 mm was maintained throughout the experiment. Flexural strength was measured using the formulae $P = 3WL/2bd^2$, where $P$ is the flexural strength, $W$ is the breaking load, $L$ is the span length; $b$ and $d$ are the width and depth of the specimens, respectively.

Table 1
Chemical analysis of raw materials (wt%).

| Constituency | Pyrophyllite | China clay | Plastic clay | Quartz | Feldspar |
|---|---|---|---|---|---|
| $SiO_2$ | 59.51 | 48.87 | 58.38 | 98.11 | 66.81 |
| $TiO_2$ | 0.26 | 0.93 | 1.15 | Trace | Trace |
| $Al_2O_3$ | 30.43 | 34.39 | 25.54 | 0.41 | 18.08 |
| $Fe_2O_3$ | 0.86 | 0.87 | 0.49 | 0.22 | 0.24 |
| Ca O | 0.37 | 1.42 | 0.95 | 0.68 | 1.03 |
| Mg O | 0.78 | Trace | Trace | Trace | 0.23 |
| $Na_2O$ | 0.73 | 0.10 | 0.13 | 0.15 | 1.69 |
| $K_2O$ | 1.95 | 0.23 | 0.63 | 0.07 | 10.94 |
| LOI | 5.40 | 12.83 | 12.24 | 0.19 | 0.58 |

Table 2
Body composition with progressive replacement of china clay with pyrophyllite (%).

| Composition | China clay | Plastic clay | Feldspar | Quartz | Pyrophyllite |
|---|---|---|---|---|---|
| P-1 | 25 | 25 | 25 | 25 | 0 |
| P-2 | 22.5 | 25 | 25 | 25 | 2.5 |
| P-3 | 20 | 25 | 25 | 25 | 5 |
| P-4 | 17.5 | 25 | 25 | 25 | 7.5 |
| P-5 | 15 | 25 | 25 | 25 | 10 |
| P-6 | 12.5 | 25 | 25 | 25 | 12.5 |
| P-7 | 10 | 25 | 25 | 25 | 15 |

Major crystalline phases present in the matured specimens were identified by X-ray diffraction (XRD) using a Philips PW-1730 X-ray diffractometer. Microstructure was studied by SEM analysis on some selected sintered samples using a LEO S-430i apparatus. SEM studies were performed on fired and matured specimens, polished and etched (using 5% HF for 60 s duration).

Concentration of crystalline phases was estimated by X-ray diffractometry in a Philips make X-pert Pro diffraction unit attached with secondary monochromator automatic divergence slit and Ni-filter was used to get monochromatic Cu Kα radiation. The instrument was run in step scan mode with step size (0.02) and time per step 8 s/step within the angle 5–75°. The collected data were refined using profit software. X-Pert plus and Quaser software based on Rietveld were used to calculate the percentage of mullite and quartz phases where standard mullite and quartz were used as reference materials.

## 3. Results and discussion

The chemical analysis (Table 1) shows that clay, quartz and feldspar used in the present study were of the common type. In the pyrophyllite sample $SiO_2$ and $Al_2O_3$ are the major constituents with low $Fe_2O_3$ and alkali ($K_2O + Na_2O$) content. The XRD pattern of pyrophyllite (Fig. 1) shows, in addition to the presence of pyrophyllite as the major phase, some quartz inclusions. The oxide compositions of all the experimental bodies are given in Table 3. The results revealed that there was

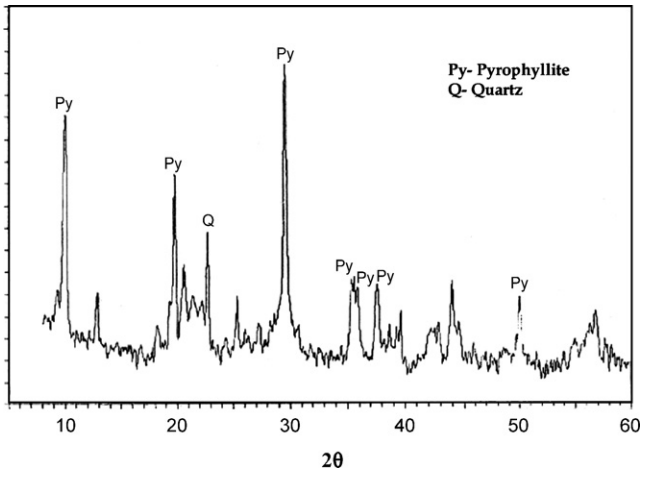


Fig. 1. XRD analysis of pyrophyllite.

Table 3
Oxide composition of the different compositions (wt%).

| Constituents | Composition | | | | | | |
|---|---|---|---|---|---|---|---|
| | P-1 | P-2 | P-3 | P-4 | P-5 | P-6 | P-7 |
| $SiO_2$ | 72.285 | 72.445 | 72.605 | 72.765 | 72.925 | 73.085 | 73.245 |
| $TiO_2$ | 0.60 | 0.58 | 0.56 | 0.54 | 0.52 | 0.50 | 0.48 |
| $Al_2O_3$ | 21.88 | 21.69 | 21.50 | 21.31 | 21.12 | 20.93 | 20.74 |
| $Fe_2O_3$ | 0.51 | 0.51 | 0.51 | 0.51 | 0.50 | 0.50 | 0.50 |
| CaO | 1.11 | 1.08 | 1.05 | 1.02 | 0.99 | 0.96 | 0.93 |
| MgO | 0.06 | 0.08 | 0.10 | 0.12 | 0.14 | 0.16 | 0.18 |
| $Na_2O$ | 0.53 | 0.55 | 0.56 | 0.58 | 0.59 | 0.61 | 0.62 |
| $K_2O$ | 3.03 | 3.075 | 3.120 | 3.165 | 3.21 | 3.265 | 3.31 |
| $SiO_2$:$Al_2O_3$ | 3.304 | 3.340 | 3.377 | 3.414 | 3.453 | 3.492 | 3.532 |

marginal increase in $SiO_2$ and decrease in $Al_2O_3$ content among the compositions (P-1 to P-7) when china clay was progressively replaced by pyrophyllite. Fig. 2a indicates that the $SiO_2/Al_2O_3$ ratio increased gradually as pyrophyllite was progressively incorporated as a replacement of china clay, however, the change was within a narrow range from 3.304 in mix P-1 to 3.532 in mix P-7. Marginal increment in alkali content was observed (varying from 3.56% to 3.93%) as more and more pyrophyllite was incorporated in the mixes (Fig. 2b), however, there was virtually no variation in the alkaline earth oxide content among the mixes. Fig. 3 shows that up to 1200 °C fired shrinkage increased with increasing pyrophyllite content, however, at higher temperature although the fired shrinkage was more as expected, but the same was found to be independent of variation in pyrophyllite content. Similar trend was also observed when quartz was progressively replaced by

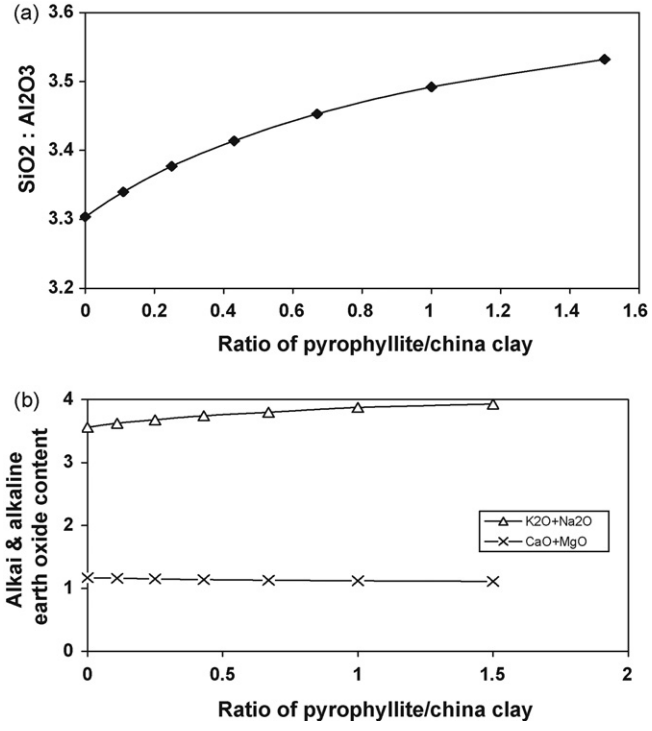


Fig. 2. (a) Variation of silica–alumina ratio with increasing pyrophyllite/china clay ratio. (b) Variation of alkali and alkaline earth oxide content with increasing pyrophyllite/china clay ratio.

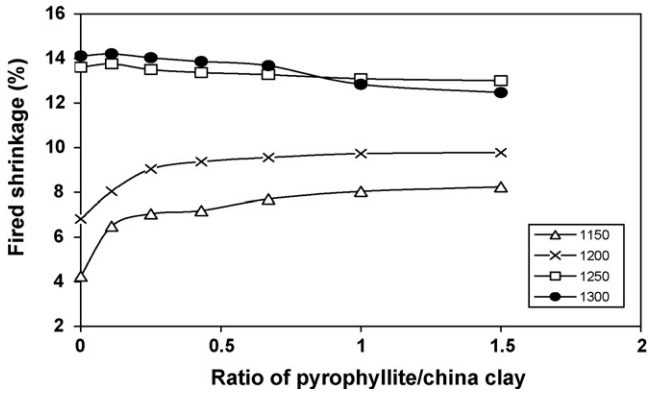


Fig. 3. Effect pyrophyllite/china clay ratio on fired shrinkage at different temperatures.

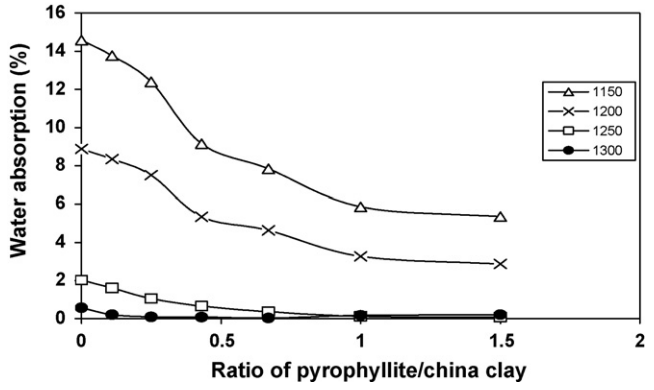


Fig. 4. Effect of pyrophyllite/china clay ratio on water absorption at different temperatures.

pyrophyllite [15]. The curve for water absorption values of specimens (Fig. 4) indicates a gradual decrease irrespective of firing temperatures when china clay was progressively replaced by pyrophyllite. Thus incorporation of pyrophyllite as a replacement of china clay in a conventional whiteware body resulted in lowering its vitrification temperature. It is interesting to note that addition of pyrophyllite (which does not contain much alkali) in the present study decreased the porosity which may be due to the formation of dense, interlocked structure during vitrification. This has also been observed by Bhasin et al. [13]. However, presence of high percentage of quartz (25%) possibly did not allow the specimens to attain complete vitrification (water absorption value <0.5%) below 1250 °C. Variation in flexural strength of fired specimens with pyrophyllite/china clay ratio has been presented in Fig. 5. It is interesting to note that MOR values gradually increased as more and more pyrophyllite was incorporated in the mixes as a replacement of china clay and fired up to 1250 °C. However, highest strength (82.7 MPa) was observed with specimen P-3 at 1300 °C with pyrophyllite/china clay ratio 0.25. There was marginal decrease in MOR value with further increase in pyrophyllite content beyond 7.5%. However, in all the cases pyrophyllite incorporated compositions produced higher MOR in comparison to that of the conventional one, i.e. mix P-1. Variation in bulk density with

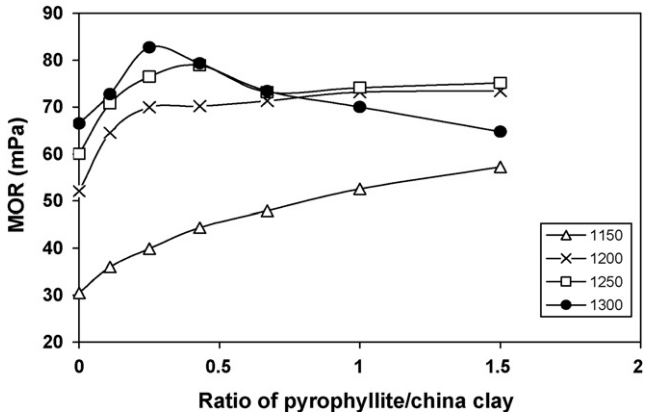


Fig. 5. Effect of pyrophyllite/china clay ratio on MOR at different temperatures.

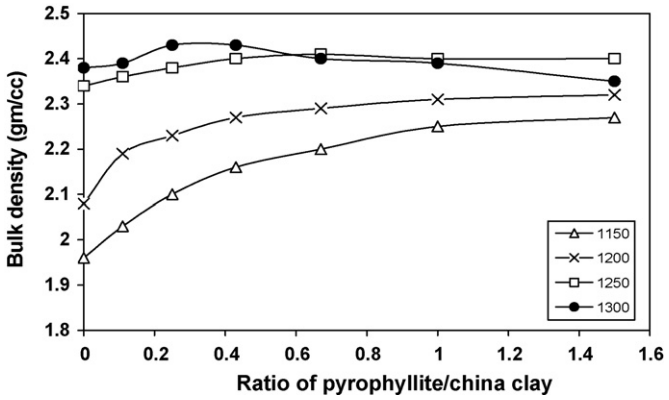


Fig. 6. Effect of pyrophyllite/china clay ratio on bulk density at different temperatures.

pyrophyllite content (Fig. 6) also showed the similar trend and increased with increasing pyrophyllite/china clay ratio and fired up to 1250 °C. However, specimens P-3 and P-4 showed the highest bulk density value (2.43 g/cm$^3$) at 1300 °C. The maximum bulk density was found to occur at the same temperature at which the highest MOR occurred, which was also observed by others [16]. Mixes P-6 and P-7 containing 12.5% and 15% pyrophyllite, respectively, showed substantial decrease in bulk density values at 1300 °C.

XRD analysis indicated two major phases viz. quartz and mullite in all the mixes. Interestingly no cristobalite phase was observed even at 1300 °C. Analysis of phases of all the specimens (Fig. 7a) fired at 1250 °C indicates higher proportions of mullite in comparison to that of conventional one (specimen P-1). Maximum mullite content (20.8%) was observed with specimen P-3 having pyrophyllite/china clay ratio of 0.25 (Fig. 7a) and the same decreased as more pyrophyllite was incorporated as a replacement of china clay (kaolin). However, in the specimens (P-5, P-6 and P-7) with pyrophyllite content beyond 7.5%, there were only little changes in the phase compositions (mullite content varied from 16.0% to 16.5% while quartz content varied from 26.9% to 27.3%). Similar types of observations were also observed when firing temperature was further increased to 1300 °C. Higher percentage of mullite was observed in all the fired specimens with varying proportion of pyrophyllite in comparison to that of P-1 (composition having no pyrophyllite). Probably the presence of pyrophyllite helped in producing a composition which facilitated mullite crystallization.

The dehydroxylation process of pyrophyllite may be assumed to follow the following sequence.

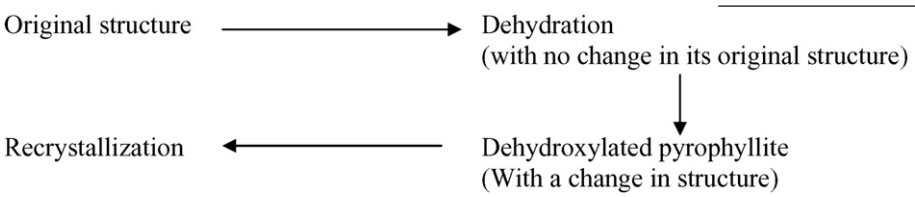


Pyrophyllite forms its anhydrous phase which is somewhat distorted in structure in comparison to that of the original one as a result of dehydroxylation. In this transformation it has been observed [17,18] that breakup of structure occurs in the direction parallel to the sheets, while the order is preserved within the sheets where only minor rearrangements take place. The entire sequence is a process in which the atomic reorganization is governed mainly by the diffusion of cations through the anion framework that has been less disturbed during the process. However, as a number of water molecules have been driven out of the crystal, this dehydroxylation process may also result in a drastic change of the entire anion framework of the crystal lattice. Nakahira and Kato [19] observed that there was little change in the entire structural scheme at the stage of dehydroxylation to form an anhydrous phase. X-ray diffraction intensities showed only lattice distortion.

The subsequent step of transformation in which mullite is formed from the dehydroxylated pyrophyllite involves a further reorganization of oxygen framework:

$$\underset{\text{Dehydroxylated pyrophyllite}}{3(Al_4Si_8O_{22})} \rightarrow \underset{\text{Mullite}}{2(3Al_2O_3, 2SiO_2)} + 20SiO_2$$

Mackenzie et al. [20] through high resolution NMR studies concluded that fully dehydroxylated pyrophylite lead to a structure containing five(5) co-ordinated Al. Wardle and Brindley [21] also observed fivefold coordination of Al in pyrophyllite dehydroxylate. Wang et al. [22] through infrared spectroscopic study observed that up to 900 °C the $SiO_4$ tetrahedral sheet structure still exists in pyrophyllite dehydroxylate, the Si–O–Al linkages and 2:1 structure remain in the dehydroxylate and that $AlO_5$ trigonal bi-pyramids form. At 1100 °C the dehydroxylate decomposes into $SiO_2$-rich amorphous phase and poorly ordered mullite. Formation of mullite from penta-coordinated dehydroxylate almost certainly involves a bonding rearrangement with simultaneous separation of silica.

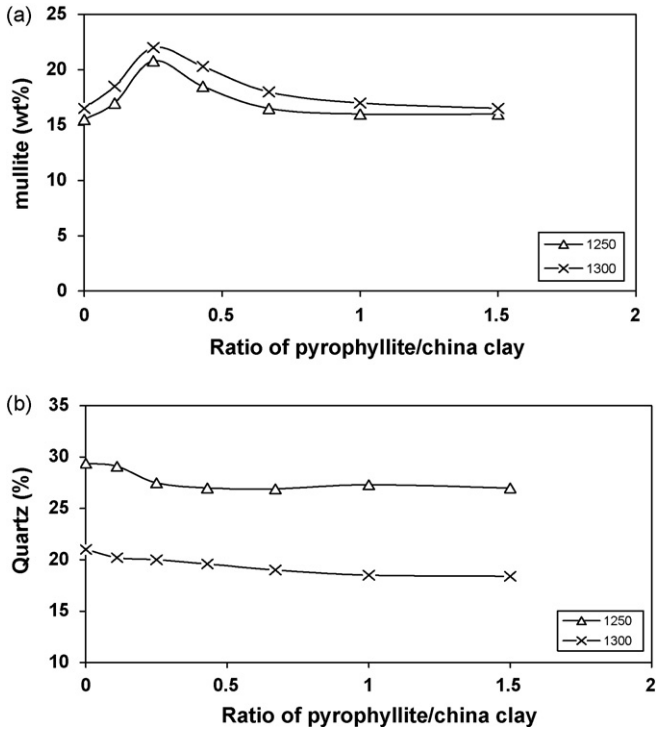


Fig. 7. (a) Effect of pyrophyllite/china clay ratio on mullitization at different temperatures. (b) Percent quartz phase present in the sintered specimens in various pyrophyllite/china clay compositions.

The structural change from dehydroxylate pyrophyllite to mullite involves the expulsion of a large amount of Si ions from those parts of the crystal where mullite is formed. This indicates that the reorganization of the oxygen framework in the dehydroxylated structure with an increase in temperature is promoted without much difficulty because of distorted open structure. The distorted open structure will provide enough space for migration of those ions.

The average mullite structure consists of chains of edge sharing $AlO_6$ octahedra running parallel to the *C*-axis. These chains are cross-linked by $(Si,Al)O_4$ tetrahedra forming double chains which also runs parallel to *C*-axis.

It is quite understandable that formation of mullite crystallization is facilitated in the presence of pyrophyllite and it may be postulated that transition of 5-coordinated Al in dehydroxylated pyrophyllite to 6-coordinated Al in mullite is rather easier. Thus in the present system, when china clay is gradually replaced by pyrophyllite, nucleation of mullite and its crystallization to form an interlocking dense microstructure is facilitated. This possibly resulted in higher percentage of mullite in specimen P3 as well as improved mechanical properties. It may be noted that simultaneously with mullite formation from dehydroxylated pyrophyllite large amount of amorphous $SiO_2$ is released which will definitely go into solution forming $SiO_2$-rich glassy phase. Beyond optimum limit, addition of pyrophyllite will result in high viscous $SiO_2$-rich glassy phase inhibiting the recrystallization of secondary mullite phase. On the contrary this glassy phase deteriorates the mechanical properties of the specimens as is observed with specimens containing more than 7.5% pyrophyllite.

Kaolinite on the other hand dehydroxylates to metakaolin where sixfold coordinated Al is transformed into fourfold coordinated Al [23]. Thermal transformation of kaolinite involves rearrangement of existing structure followed by crystallization of a new phase. The transformation of fourfold coordinated Al in $Al_2O_3$–$SiO_2$ spinel to sixfold coordinated Al in mullite requires to cross higher energy barrier and thus it is expected that under similar environment mullitization from pyrophyllite will be rather easier than that from kaolinite. This is possibly the reason for less mullite formation in specimen P1 where pyrophyllite content is zero.

Another important observation is that quartz phase content in the matured specimens at 1250 °C varied within a narrow range 26.9–29.4% (Fig. 7b). Although 25% quartz was added in all the mixes, presence of free quartz in the other materials contributed to the increased values. The quartz phase decreased substantially at 1300 °C irrespective of the specimens analysed, however, there was marginal increase in the percentage of mullite [17]. One interesting observation (Fig. 7b) is that there was hardly any variation in the quartz phase among the specimens when the pyrophyllite/china clay ratio was altered beyond 0.4 irrespective of the firing temperature 1250 °C or 1300 °C.

SEM analysis of specimen P-1 fired at 1250 °C (Fig. 8) revealed two different types of mullite; clay agglomerate relicts containing primary granular type mullite and a matrix of clay–feldspar and quartz containing elongated and acicular type mullite in agreement with the observations of Lee and Iqbal [25]. The general microstructural features of commercial porcelain have been observed, i.e. coarse quartz grains surrounded by solution rims of almost pure silica glass embedded in a much finer matrix system. Distinct cracks and fissures have been observed in the large quartz grains indicating severe strains around the grains. Quartz grains were rather large and angular in nature. These flaws were formed as a result of quartz and matrix expansion mismatch and the same determine the maximum possible strength of the porcelain as observed by Kobayashi et al. [24]. The matrix is predominantly glass of varying composition being alkali (Na,K) aluminosilicate in flux

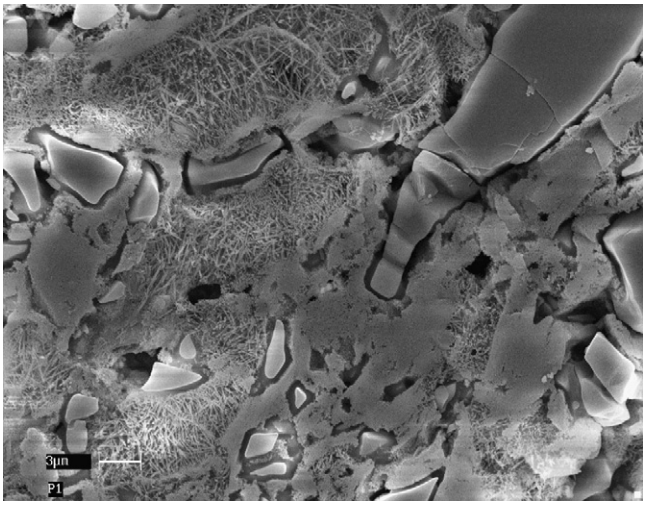


Fig. 8. SEM of composition P-1 at 1250 °C.

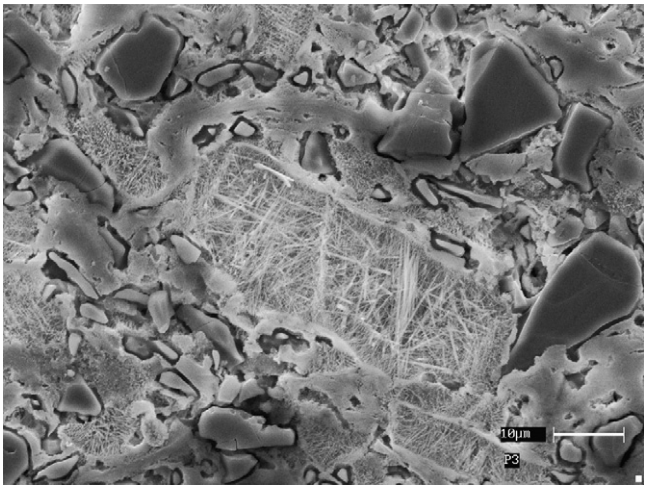


Fig. 9. SEM of composition P-3 at 1250 °C.

penetrated regions. The proportion of acicular mullite increased as more and more pyrophyllite was incorporated. Figs. 9 and 10 (SEM of P-3 and P-4, respectively fired at 1250 °C) show well formed needle shaped secondary mullite forming a network throughout the microstructure. In concurrence with the observations of Iqbal and Lee [25,26] two different types of secondary mullite crystals were observed. One variety (Type III) with very high aspect ratio (30–40/1) and the second one of Type II with lower aspect ratio (3–10/1) in feldspar penetrated clay relicts. The elongated Type III mullite crystals occur in regions also containing Type II and were associated with a fluid matrix. The elongated type mullite crystals were very prominent in the microstructure of specimens P-3 and P-4 containing 5% and 7.5% pyrophyllite, respectively. The observed variation in the morphology and the size of mullite crystals may be explained by the gradient in viscosity of the relevant matrix and subsequent more rapid mass transport [27]. Table 3 indicated that as pyrophyllite gradually replaced china clay in the mixes, total alkali ($Na_2O + K_2O$) and $SiO_2$ content increased progressively while there was a gradual decrease in the $Al_2O_3$ content and this resulted in decrease in viscosity of

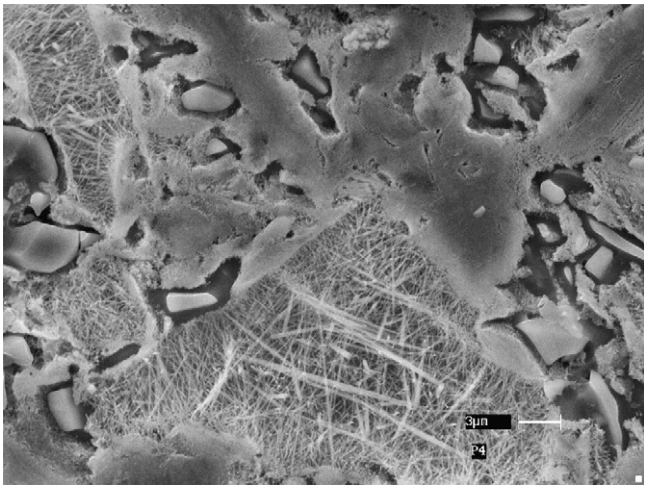


Fig. 10. SEM of composition P-4 at 1250 °C.

Table 4
Phase analysis (wt%) of specimens of the different compositions fired at 1250 °C and 1300 °C.

| Composition | Mullite | | Quartz | | Glass | |
|---|---|---|---|---|---|---|
| | 1250 °C | 1300 °C | 1250 °C | 1300 °C | 1250 °C | 1300 °C |
| P-1 | 15.5 | 16.5 | 29.4 | 21.0 | 55.1 | 62.5 |
| P-2 | 17.0 | 18.5 | 29.1 | 20.2 | 53.9 | 61.3 |
| P-3 | 20.8 | 22.0 | 27.5 | 20.0 | 51.7 | 58.0 |
| P-4 | 18.5 | 20.3 | 27.0 | 19.6 | 54.5 | 60.1 |
| P-5 | 16.5 | 18.0 | 26.9 | 19.0 | 56.6 | 63.0 |
| P-6 | 16.0 | 17.0 | 27.3 | 18.5 | 56.7 | 64.5 |
| P-7 | 16.0 | 16.5 | 27.0 | 18.4 | 57.0 | 65.1 |

the glassy phase. The increase in fluidity of the matrix resulted in enhancing the size of secondary mullite (Type III) and thus supports the observations of Lee and Iqbal [25]. The relatively higher proportion of mullite and its well developed interlocking network structure distributed throughout the matrix in the specimens of P-3 and P-4 contributed significantly to the development of higher flexural strength (Fig. 5). As the relative proportion of pyrophyllite was increased in the mixes the quartz grains tend to become round and smaller in sizes. The wide solution rims around quartz grains showed their extensive dissolution. It may be revealed from Table 4 that proportion of glassy phase varied within a narrow range 51.7% (specimen P-3) to 57.0%(specimen P-7) at 1250 °C and the same increased significantly when temperature was further increased to 1300 °C showing a maximum value of 65.1% for specimen P-7. Composition of probable glassy phase present in different mixes has been presented in Table 5. It reveals from the results that viscosity of the glassy phase of mixes P-3 and P-4 would be rather on the lower side in comparison to those of other mixes and thus facilitating the recrystallization of secondary mullite and its growth to type III with high aspect ratio. This in turn supports the results of Fig. 7a. Increased strength and toughness have been reported in porcelains containing increased amounts of high aspect ratio mullite [28]. This also supports the observed results presented in Fig. 5. As percentage of pyrophyllite went beyond 7.5% in the mixes (P-5, P-6 and P-7) the glass/crystal ratio as well as the composition of the glassy phase remained more or less constant and this has been reflected in the microstructure of the three specimens. In the microstructure of specimens P-6 and P-7 (Figs. 11 and 12) fired at 1250 °C, predominance of type II mullite is observed. Presence of both angular as well as round-shaped quartz grains

Table 5
Calculated composition of probable glassy phase present in different compositions (wt%) at 1250 °C (considering mullite as $3Al_2O_3{\cdot}2SiO_2$).

| Composition | $SiO_2$ | $Al_2O_3$ | $Na_2O + K_2O$ | CaO | MgO | $Fe_2O_3$ | $TiO_2$ |
|---|---|---|---|---|---|---|---|
| P-1 | 69.89 | 19.51 | 0.96 + 5.50 | 2.01 | 0.11 | 0.93 | 1.09 |
| P-2 | 71.52 | 17.58 | 1.02 + 5.70 | 2.00 | 0.15 | 0.95 | 1.08 |
| P-3 | 75.90 | 12.69 | 1.08 + 6.03 | 2.03 | 0.19 | 0.99 | 1.08 |
| P-4 | 74.40 | 14.71 | 1.06 + 5.81 | 1.87 | 0.22 | 0.94 | 0.99 |
| P-5 | 73.11 | 16.38 | 1.04 + 5.67 | 1.75 | 0.25 | 0.88 | 0.92 |
| P-6 | 72.78 | 16.65 | 1.08 + 5.76 | 1.69 | 0.28 | 0.88 | 0.88 |
| P-7 | 73.21 | 16.23 | 1.09 + 5.81 | 1.63 | 0.32 | 0.88 | 0.84 |

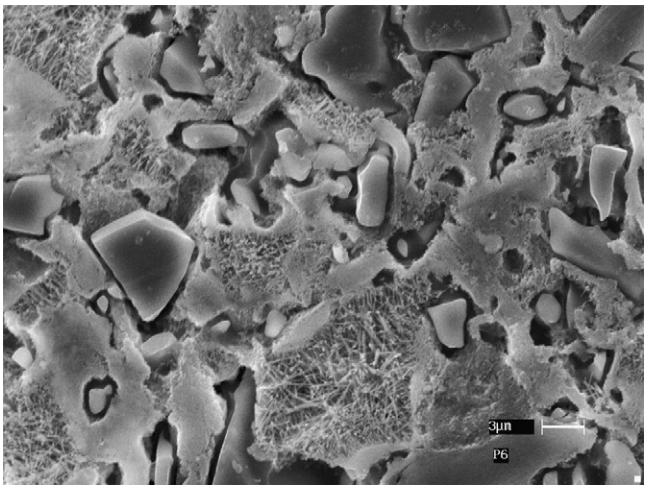


Fig. 11. SEM of composition P-6 at 1250 °C.

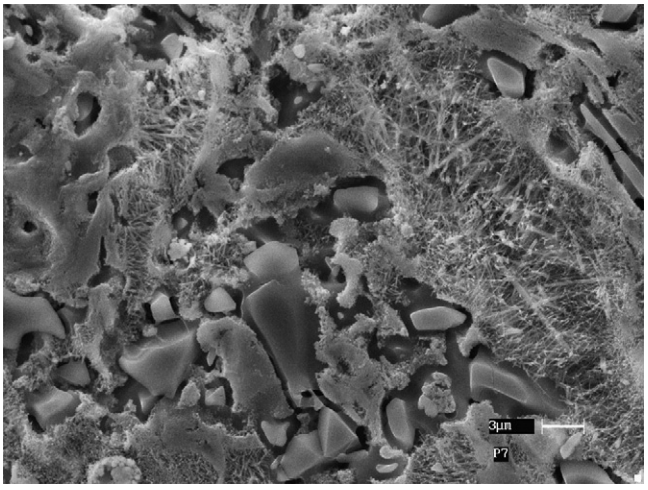


Fig. 12. SEM of composition P-7 at 1250 °C.

is conspicuous. Large amounts of quartz remained undissolved, which may be assumed to hinder the propagation of cracks. At 1250 °C, pores were rather isolated and small. All these factors contributed positively in attaining high strength for the specimens P-5, P-6 and P-7. Same observations were made by other workers [24,29] working on similar but non-pyrophyllite systems.

## 4. Conclusions

Incorporation of pyrophyllite as a progressive replacement of china clay (kaolin) in a porcelain composition resulted in early vitrification. Addition of pyrophyllite reduced fired shrinkage and improved the flexural strength as compared to those of the conventional body due to development of interlocking mullite needles. Percentage of mullite was found to increase in the mixes while kaolinite was progressively replaced by pyrophyllite. However maximum flexural strength and mullite content were observed with mix having 5% pyrophyllite content at 1300 °C. The formation of mullite crystallization is facilitated in the presence of pyrophyllite and it may be postulated that transition of 5-coordinated Al in dehydroxylated pyrophyllite to 6-coordinated Al in mullite is rather easier in comparison to that from 4-coordinated Al in metakaolin. Incorporation of pyrophyllite in percentage higher than 7.5% resulted in deterioration in ceramic properties as well as mullite content. Beyond 7.5% pyrophyllite addition, amorphous $SiO_2$ released from pyrophyllite dehydroxylation will form $SiO_2$ rich glassy phase inhibiting further recrystallization of mullite. There was hardly any change in the phase compositions with mixes having pyrophyllite content higher than 7.5%. The size and shape of mullite crystals is to a large extent controlled by the fluidity of the liquid matrix and this is again a function of temperature and composition. Large amount of undissolved quartz was observed in all the specimens, however, their size was found to be the guiding factor in the development of ultimate strength of porcelains. Significant decrease in quartz phase was observed when temperature was raised from 1250 °C to 1300 °C, however, there was marginal increase in mullite phase. The amount of closed pores in the specimens with pyrophyllite content beyond 10% and fired at 1300 °C was found to increase very abruptly which in turn is expected to increase the mean free fracture path per unit volume resulting in a decrease in strength.

## Acknowledgement

Authors wish to acknowledge the assistance received from XRD, SEM and Analytical Chemistry sections for characterizing the samples.

## References

[1] A. Tucci, L. Esposito, E. Rastelli, C. Palmonari, E. Rambaldi, Use of sodalime scrap-glass as a fluxing agent in a porcelain stoneware tile mix, J. Eur. Ceram. Soc. 24 (1) (2004) 83–92.
[2] F. Matteucci, M. Dondi, G. Guarini, Effect of soda-lime glass on sintering and technological properties of porcelain stoneware tiles, Ceram. Int. 28 (8) (2002) 873–880.
[3] R. Gennaro, P. Cappelletti, G. Cerri, M. Gennaro, M. Dondi, G. Guarini, A. Langella, D. Naimo, Influence of zeolites on sintering and technological properties of porcelain stoneware tiles, J. Eur. Ceram. Soc. 23 (13) (2003) 2237–2245.
[4] A.P. Luz, S. Ribeiro, Use of glass waste as a raw material in porcelain stoneware tile mixtures, Ceram. Int. 33 (2007) 761–765.
[5] I. Augusto, P. Pilar, S. Fernando, P. Gonzalez, Modification of the inert component in wall-tile bodies, Am. Ceram. Soc. Bull. 71 (11) (1992) 1661–1668.
[6] M.F. Abadir, E.H. Sallam, I.M. Bakr, Preparation of porcelain tiles from Egyptian raw materials, Ceram. Int. 28 (3) (2002) 303–310.
[7] P. Appendino, M. Ferraris, I. Matekovits, M. Salvo, Production of glass–ceramic bodies from the bottom ashes of municipal solid waste incinerators, J. Eur. Ceram. Soc. 24 (2004) 803–810.
[8] M. Campos, F. Velasco, M.A. Martinez, J.M. Torralba, Recovered slate waste as raw material for manufacturing sintered structural tiles, J. Eur. Ceram. Soc. 24 (2004) 811–819.
[9] V.K. Marghussian, A. Maghsoodipoor, Fabrication of unglazed floor tiles containing Iranian copper slags, Ceram. Int. 25 (1999) 617–622.
[10] T.K. Mukhopadhyay, T.K. Dan, Energy conservation in whiteware industry—the Indian scenario, J. Sci. Ind. Res. 55 (February) (1996) 73–85.
[11] H. Moertel, Influence of the batch composition on the reaction behaviour and properties of fast fired (2 h) porcelain, Sci. Ceram. 9 (1977) 84–91.

[12] C.S. Prasad, K.N. Maiti, R. Venugopal, Replacement of quartz and potash feldspar with sericitic pyrophyllite in whiteware compositions, Interceram 40 (2) (1991) 94–98.
[13] S. Bhasin, S.S. Amritphale, S. Chandra, Effect of pyrophyllite addition on sintering characteristics of fly ash based ceramic wall tiles, Br. Ceram. Trans. 102 (2) (2003) 83–86.
[14] C.K. Rieger, Pyrophyllite, Am. Ceram. Soc. Bull. 71 (1992) 813.
[15] T.K. Mukhopadhyay, S. Ghosh, S. Ghatak, H.S. Maiti, Effect of pyrophyllite on vitrification and on physical properties of triaxial porcelain, Ceram. Int. 32 (2006) 871–876.
[16] S.R. Braganca, C.P. Bergmann, A view of whitewares mechanical strength and microstructure, Ceram. Int. 29 (2003) 801–806.
[17] W.F. Bradley, R.E. Grim, High temperature thermal effects of clay and related materials, Am. Miner. 36 (1951) 182–201.
[18] L. Heller, V.C. Farmer, R.C. Mackenzie, B.D. Mitchell, H.F.W. Taylor, The dehydroxylation and rehydroxylation of triphormic dioctahedral clay minerals, Clay Miner. Bull. 5 (1962) 56–72.
[19] M. Nakahira, T. Kato, Thermal transformations of pyrophyllite and talc as revealed by X-ray and electron diffraction studies, Proceedings of the Twelfth National Conference on Clays and Clay minerals, Contribution No. 63-53, in: W.F. Bradley (ed.), College of Mineral Industries, The Pennsylvania State University, Pennsysvania, Pergamon Press, New York, 1964, pp. 21–27.
[20] K.J.D. Mackenzie, I.W.M. Brown, R.H. Meinhold, M.E. Bowden, Thermal reactions of pyrophyllite studied by high-resolution solid-state $^{27}$Al and $^{29}$Si nuclear magnetic resonance spectroscopy, J. Am. Ceram. Soc. 68 (5) (1985) 266–272.
[21] R. Wardle, G.W. Brindley, The crystal structure of pyrophyllite, 1Tc, and of its dehydroxylate, Am. Miner. 57 (1972) 732–750.
[22] L. Wang, M. Zhang, S.A.T. Redfern, Z. Zhang, Dehydroxylation and transformation of the 2:1 phyllosilicate pyrophyllite at elevated temperatures: an Infra red Spectroscopic study, Clays and Clay Miner. 50 (2) (2002) 272–283.
[23] M.C. Gastuche, F. Toussaint, J.J. Fripiat, R. Touilleaux, M. Van Meersche, Study of intermediate stages in the kaolin–metakaolin transformation, Clay Miner. 5 (29) (1963) 227–236.
[24] Y. Kobayashi, O. Ohira, Y. Ohashi, E. Kato, Effect of firing temperature on bending strength of porcelains for tableware, J. Am. Ceram. Soc. 75 (7) (1992) 1801–1806.
[25] W.E. Lee, Y. Iqbal, Influence of mixing on mullite formation in porcelain, J. Eur. Ceram. Soc. 21 (2001) 2583–2586.
[26] I. Yaseen, E. William Lee, Fired porcelain microstructures revisited, J. Am. Ceram. Soc. 82 (12) (1999) 3584–3590.
[27] W.M. Carty, U. Senapati, Porcelain—raw materials, processing, phase evolution, and mechanical behaviour, J. Am. Ceram. Soc. 81 (1) (1998) 3–20.
[28] S.P. Chaudhuri, Ceramic properties of hard porcelain in relation to mineralogical composition and microstructure. VI. Thermal shock resistance and thermal expansion, Trans. Ind. Ceram. Soc. XXXIV (1) (1975) 30–34.
[29] R.C. Bradt, A high-tech approach to a traditional ceramic—the toughness of porcelain, in: Proceedings of International Symposium on fine Ceramics Arita, vol. 86, 1986, pp. 15–22.